Proceedings of IMECE 2004
2004 ASME International Mechanical Engineering Congress
Anaheim, California, USA, November 13-19, 2004

IMECE2004-60129

EXPERIMENTAL AND ANALYTICAL INVESTIGATION OF COMPACT LIQUID COOLED HEAT SINKS

M. Zugic[⋆] **, J. R. Culham**[†] **, P. Teertstra**[‡]
Department of Mechanical Engineering
University of Waterloo
Waterloo, ON, Canada N2L 3G1
Email: maja@mhtlab.uwaterloo.ca
rix@mhtlab.uwaterloo.ca
pmt@mhtlab.uwaterloo.ca

Y. Muzychka[§]
Faculty of Engineering
and Applied Science
Memorial University of Newfoundland
St. John's, NL, Canada A1B 3X5
Email: yuri@engr.mun.ca

K. Horne, E. Knapp, J-F. de Palma
Ferraz Shawmut Inc.
374 Merrimac St.
Newburyport, MA 01950

ABSTRACT

Compact, liquid cooled heat sinks are used in applications where high heat fluxes and boundary resistance preclude the use of more traditional air cooling techniques. Four different liquid cooled heat sink designs, whose core geometry is formed by overlapped ribbed plates, are examined. The objective of this analysis is to develop models that can be used as design tools for the prediction of overall heat transfer and pressure drop of heat sinks. Models are validated for Reynolds numbers between 300 and 5000 using experimental tests. The agreement between the experiments and the models ranges from 2.35% to 15.3% RMS.

NOMENCLATURE

A	cross sectional area, m^2
A_{ch}	channel cross sectional area $\equiv b^2$, m^2
b	side of square channel $\equiv 6.35\ mm$
C_p	fluid heat capacity, $J/(kg \cdot K)$
D_h	hydraulic diameter $\equiv 4A/P$, m
f	Fanning friction factor $\equiv \overline{\tau}_w/(\frac{1}{2}\rho\overline{V}^2)$
$\overline{h}$	heat transfer coefficient, $W/(m^2 \cdot K)$
K	local loss coefficient $\equiv \Delta p/(\frac{1}{2}\rho\overline{V}^2)$
k_1	correction factor
L_{ch}	channel length, pressure drop model, m
l_{ch}	channel length, heat transfer model, m
N	number of channels in the core
Δp	pressure drop, Pa
Q	total heat transfer rate, W
t	time, s
T_i	i-th temperature at heat sink interface, K
T_{in}, T_{out}	fluid inlet/outlet temperature, K
ΔT_{lm}	log-mean temperature difference, K
T_S	heat sink UWT, K
UWT	uniform wall temperature
$\dot{V}$	volumetric flow rate, m^3/s

Greek Symbols

δ	angle of fluid turn, *degrees*
μ	dynamic viscosity, $N \cdot s/m^2$
ρ	density, kg/m^3
$\overline{\tau}_w$	wall shear stress, N/m^2

Subscripts

app	apparent
C	contraction

[⋆] Graduate Research Assistant

[†] Associate Professor, Director, Microelectronics Heat Transfer Laboratory

[‡] Research Assistant Professor

[§] Assistant Professor

ch	channel
δ	fluid δ turn
E	expansion
exp	experimental
fitt	inlet/outlet fitting
pl	plenum
tot	total

INTRODUCTION

The thermal performance of liquid cooled heat sinks is of particular interest in the thermal management of electronic devices such as IGBTs that dissipate high power, e.g. of order 1 *kW* or more. Since the geometry of a compact heat sink greatly effects its thermal and hydrodynamic performance, the optimization of the internal flow passage design to enhance heat transfer and reduce pressure drop represents a significant design challenge.

The objective of this study is the experimental testing and analytical modeling of pressure drop and heat transfer for a novel liquid cooled heat sink design. The unique internal geometry of the heat sink represents a commercial design that balances heat transfer performance with minimal pressure drop while maintaining good manufacturability. A review of the literature reveals no previous work that directly relates to the particular geometry of the present study. The work of Baumann et al. [1] is most closely related to the present investigation of liquid cooled cold plate performance. It numerically explores the design modifications of a pin – array heat sink, including the size and shape of the plenums. Agonafer, Han and Schmidt [2] present a numerical study of heat transfer and pressure drop in a cold plate with serpentine channels. There are also studies such as those by Stasiek et al. [3], Ciofalo et al. [4], Focke et al. [5], Okada et al. [6], Blomerius et al. [7], Rosenblad et al. [8] and Croce et al. [9] that consider the flow pattern formed by crossed corrugated (sinusoidal) plates, which is similar to the core of the heat sinks in the current study. These researchers were mainly concerned with the experimental and numerical studies of the effect of the crossing angle between the channels and the pitch-to-height ratio on the heat transfer and pressure drop of the corrugated section, lacking a more general analytical consideration.

The present work will develop models to predict the heat transfer and pressure drop for this particular design of compact heat sinks, and the model predictions will be compared with experimental tests conducted on four different geometries.

EXPERIMENTAL MEASUREMENT

Four heat sink designs having similar basic design features were used in the experimental test program. Each heat sink consists of two identical ribbed plates that, when brazed together, form a complex inner geometry that consists of the core, two plenums and the barb connectors, as shown in Fig. 1. The inlet and the outlet in heat sinks A and C are aligned, while heat sinks B and D have the inlet and outlet positioned in parallel. The inclination angle of the channels on the two halves of the heat sink, with respect to each other, is 60°. The channel cross section dimensions of 6.35 *mm* × 6.35 *mm* are the same for all four heat sinks. The shapes of the inlet and the outlet plenums are identical, and each have the same height of 2×6.35 *mm* (12.7 *mm*). The experimental investigations for thermal performance and pressure drop were performed separately, i.e. the heating was not applied in the pressure drop measurements. All tests used the same fluid, a 50/50 (volume based) ethylene glycol/water mixture. The schematic of the test apparatus is shown in Fig. 2.

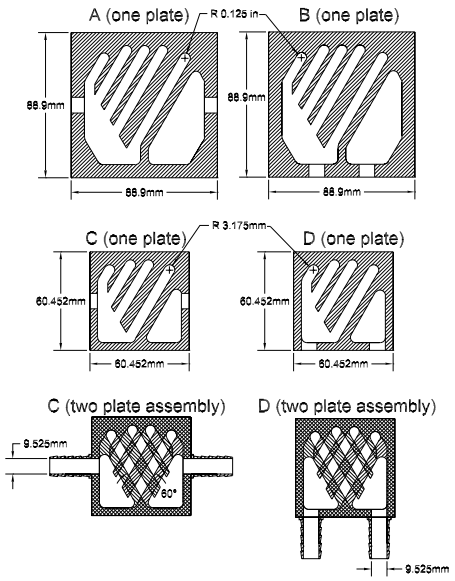

Figure 1. TESTED HEAT SINKS

Hydrodynamic Tests

The steady state pressure drop was tested in the following conditions:

1. volumetric flow rate range: 9.46 - 2.27 $L/$ min, in steps of 0.378 $L/$ min
2. constant fluid temperature: 15, 21, 27°C.

The measurements of the steady state pressure drop were obtained using a differential pressure transducer ($0 - 68.95$ *kPa*) whose taps were positioned in the inlet and outlet hoses, about 15 cm from the barb fittings ($\Delta p_{\text{heat sink+system}}$). Additional measurements of the system pressure drop without the heat sink were done (Δp_{system}) to be able to subtract the pressure drop that occurred in the hoses and calculate the heat sink pressure drop alone (Δp_{tot}):

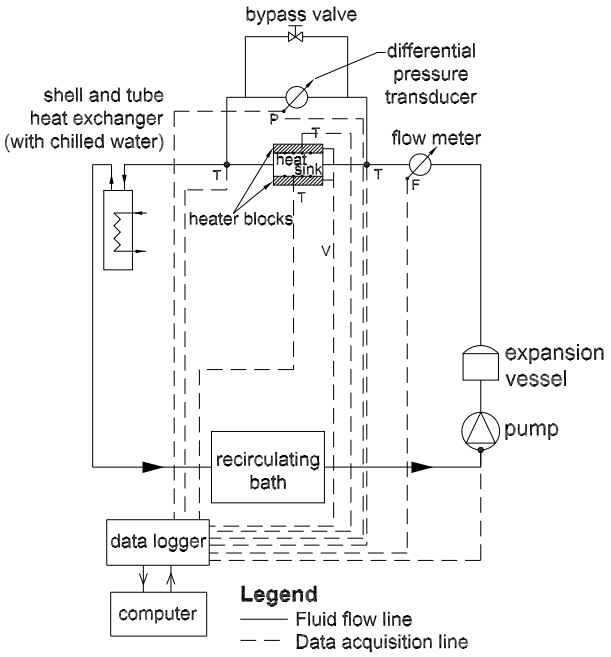

Figure 2. SCHEMATICS OF EXPERIMENTAL APPARATUS (T-TEMPERATURE, P- PRESSURE, F- FLOWRATE, V- VOLTAGE)

$$\Delta p_{tot} = \Delta p_{\text{heat sink+system}} - \Delta p_{\text{system}} \tag{1}$$

The steady state criterion in the pressure tests required the collection of 20 pressure readings between the desired flow rates, with a measurement tolerance of $\pm 0.0378\ L/\min$. The repeatability of the experimental tests, validated by several repetitions, is within $\pm 5\%$.

Thermal Tests

The test procedure for the heat transfer experiments was based on determining the mean, steady state temperature of the calistor for varying flow rates at certain heat loads and contact pressures. The cold plates were heated symmetrically and uniformly by two aluminum heater blocks supplied with embedded cartridge heaters. Each heater block contained five cartridge heaters connected in parallel providing a heat capacity of $\approx 150W$ per cartridge heater. In order to maintain a repeatable interface pressure between the heater blocks and the heat sink a loading apparatus consisting of a 19.62 kN hydraulic press with a 9.81 kN load cell was used to apply a uniform and repeatable load of $\cong 4.005\ kN$ to the calistor – heater block assembly. The temperatures on the top and the bottom heat sink surfaces were measured using eight T type thermocouples, four for each side, located at the circular surface of the copper adaptor, as shown in Fig. 3. The thermocouples were distributed such that an arithmetic mean would capture the average surface temperature on

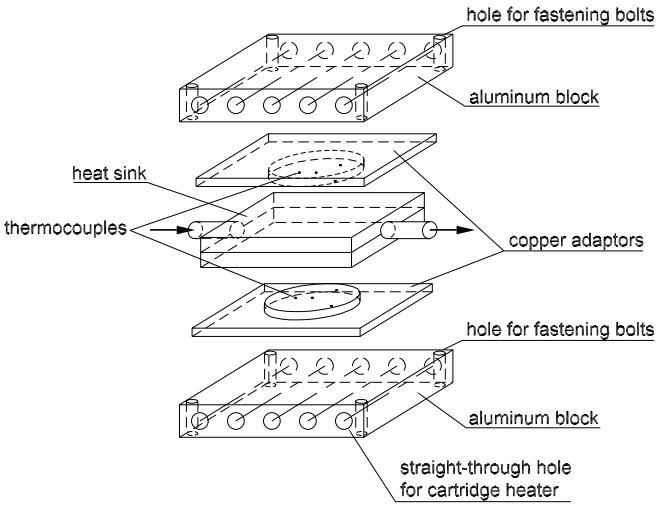

Figure 3. HEAT SINK - COPPER ADAPTOR - HEATER BLOCK ASSEMBLY

the heat sink. In order to reduce the contact resistance, a thin layer of thermal grease was applied at the heat sink – copper adaptor interface. Bearing in mind that the heat sinks are made of copper, the thermal resistance through the wall is considered negligible. To reduce the heat loss to the surroundings the calistor – heater blocks assembly was wrapped in approximately 10 cm fiberglass insulation. The estimated heat loss to the surroundings, verified by measurements, is approximately 15 - 20 %. The inlet and outlet temperature of the fluid were measured using two T type thermocouple probes inserted into fittings located before and after the heat sink.

The procedure for thermal testing was as follows:

1. set volumetric flow rate range ($9.46 - 1.89\ L/\min$, in steps of $0.757\ L/\min$)
2. set the constant overall heat load ($\cong 1500W$)
3. record the steady state measurements at desired flow rate.

For each flow rate, the steady state measurements were determined using the following criterion:

$$\frac{\left|(T_S - T_{in})_{t+\Delta t} - (T_S - T_{in})_t\right|}{\Delta t} \leq 0.0005 \tag{2}$$

$$\Delta t = 6s \text{ (sampling rate)};\ T_S = \frac{\sum_{i=1}^{8} T_i}{8} \tag{3}$$

The steady state value was an arithmetic average of 20 consecutive data points which fulfilled the criterion above. The repeatability of the thermal tests has shown to be within $\pm 7\%$.

In order to consider only heat transfer between the heater plates and the heat sink, an enthalpy balance for the fluid was

used to calculate the total heat transfer rate, Q, and the experimental heat transfer coefficient, $h_{tot-\exp}$:

$$Q = \rho \dot{V} C_p (T_{out} - T_{in}) \tag{4}$$

$$h_{tot-\exp} = \frac{\rho \dot{V} C_p (T_{out} - T_{in})}{A_{tot} \Delta T_{lm}}, [W/(m^2 K)] \tag{5}$$

where the log-mean temperature difference, ΔT_{lm}, is defined as:

$$\Delta T_{lm} = \frac{T_{out} - T_{in}}{\ln\left(\frac{T_S - T_{in}}{T_S - T_{out}}\right)}, [K] \tag{6}$$

The heat transfer from the heat sink to the surroundings is assumed to be negligible, which provides a conservative estimate of the total heat transfer between the heat source and the coolant.

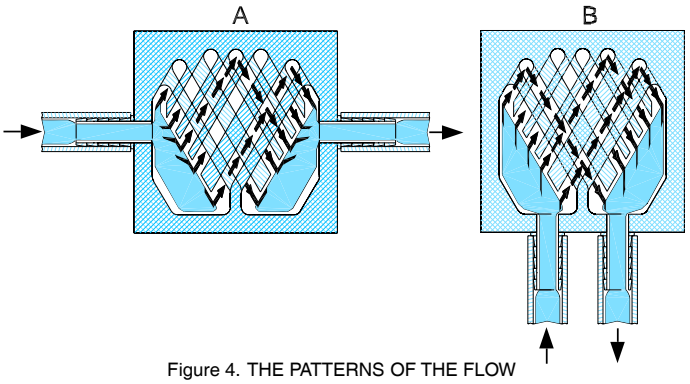

Figure 4. THE PATTERNS OF THE FLOW

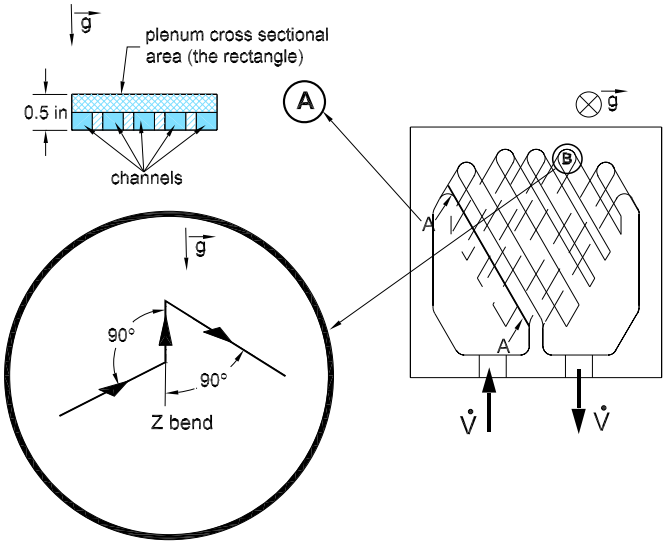

Figure 5. DETAIL A: THE SUDDEN CONTRACTION FROM THE PLENUM TO THE CHANNELS; DETAIL B: Z BEND

All the fluid properties are evaluated at the average fluid temperature $T_m = (T_{in} + T_{out})/2$. Heat transfer and pressure drop data for each of the four heat sink configurations are presented with model validation in subsequent sections.

MODEL DEVELOPMENT

Analytical models are developed that predict pressure drop and heat transfer for heat sinks A, B, C and D.

Hydrodynamic Model

The pressure drop in the heat sink is modeled based on a hydraulic resistance network that consists of all significant pressure losses encountered in the flow path. Based on the inner geometry of the heat sinks, flow patterns are deduced for the different inlet and outlet positions, as shown in Fig. 4. Based on this assumed flow pattern, major pressure losses in the system are:

1. sudden contraction from the $\phi 12.7$ *mm* tubing to the $\phi 9.525$ *mm* barb fitting, Δp_{C-fitt}
2. sudden expansion from the barb fitting to the inlet plenum, Δp_{E-pl}
3. change in direction of the flow from/to the plenum when entering/exiting the core channels, $\Delta p_{\delta-turn}$
4. sudden contraction from the 12.7 *mm* high plenum to the 6.35 *mm* high core channels, Δp_{C-ch} (Fig. 5, detail A)
5. friction loss along the channels, Δp_{ch}
6. Z turn (two 90° bends) between the bottom and the top plate channels, Δp_{Z-bend} (Fig. 5, detail B)
7. sudden expansion from the 6.35 *mm* high core channels to the 12.7 *mm* high plenum, Δp_{E-ch}
8. sudden contraction from the plenum to the barb fitting, Δp_{C-pl}
9. sudden expansion from the $\phi 9.525$ *mm* barb fitting to the $\phi 12.7$ *mm* tubing, Δp_{E-fitt}.

The above listed sudden changes of the flow area and direction and the viscous shear (wall friction) present the hydraulic resistances causing irreversible pressure losses, shown in Fig. 6. The flow distribution from the inlet plenum to the channels of the core is assumed uniform. It is also assumed that once the fluid enters the square ducts in the core, it flows along the channel without mixing with the fluid from other channels, and has a continuous channel flow of length L_{ch} and of constant cross sectional area $A_{ch} = b^2 = (6.35\ mm)^2$ (Fig. 7). Since the channel lengths (L_{ch}) in the heat sink are close but not identical, one averaged value represents all. Figure 7 also shows the difference in the angle of the fluid turn (δ) for the heat sink with the aligned fittings ($\delta = 120°$) and with the parallel fittings ($\delta = 30°$).

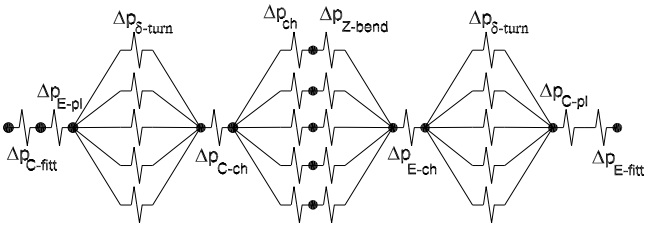

Figure 6. HYDRAULIC RESISTANCE NETWORK

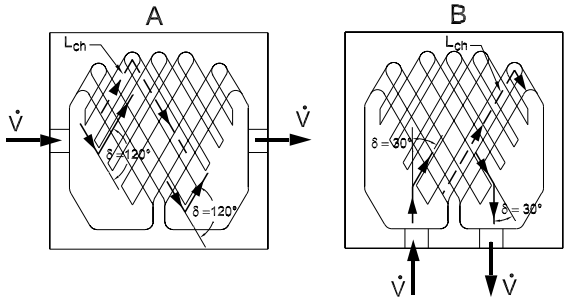

Figure 7. THE CHANNEL LENGTH AND THE ANGLES FOR FLUID TURN

According to the hydraulic resistance network, the total pressure drop across the heat sink is:

$$\Delta p_{tot} = \Delta p_{C-fitt} + \Delta p_{E-pl} + 2\cdot\Delta p_{\delta-turn} + \Delta p_{C-ch} + \Delta p_{ch} + \Delta p_{Z-bend} + \Delta p_{E-ch} + \Delta p_{C-pl} + \Delta p_{E-fitt} \quad (7)$$

Pressure Drop Relationships for Model In order to find the overall pressure drop, the pressure losses in Eq. (7) are required. Idelchik [10], Blevins [11] and White [12] provide the relations for the local losses due to sudden changes of the flow area or flow direction. The friction loss through the channel L_{ch} (Δp_{ch}) was determined using the model developed by Muzychka [13].

The local loss coefficients of a sudden contraction (K_C) ([12], [11]) and expansion (K_E) [10] are:

$$K_C = \frac{\Delta p_C}{\frac{1}{2}\rho V_0^2} = k_1\left[\frac{38}{Re_0} + 0.42\left(1-\frac{F_0}{F_1}\right)\right] \quad (8)$$

$$K_E = \frac{\Delta p_E}{\frac{1}{2}\rho V_0^2} = k_1\left[\frac{30}{\mathrm{Re}_0} + \left(1-\frac{F_0}{F_1}\right)^2\right] \quad (9)$$

$$\mathrm{Re}_0 = \frac{\rho d_0 V_0}{\mu} \quad (10)$$

where F_0 and F_1 are the smaller and larger cross sectional areas, d_0 is smaller (equivalent) diameter and V_0 is mean velocity through d_0. The equivalent diameter of non-circular duct is defined as the square root of cross sectional area, according to Muzychka ([13], [14]), whose Fanning friction factor and Nusselt number model for the plain duct flow were used in the modeling process of the current study. The factor $k_1 \leq 1$ is a correction factor for the asymmetric cases of sudden expansion/contraction in rectangular ducts and it depends on the aspect ratio of the channel width and height (B/H) [10]. The values of k_1 for the tested heat sinks are shown in Table 1.

The $\Delta p_{\delta-turn}$ loss as the flow enters/exits the core is modeled as a sharp elbow with constant square cross sectional area of A_{ch}. The local loss coefficient for the sharp square elbows is a function of the angle of the fluid turn, δ [10]:

$$K_\delta = \frac{\Delta p_{\delta-turn}}{\frac{1}{2}\rho V_\delta^2} = (k_{\delta 1}+1)\cdot 0.97\cdot\left[\left(0.95+\frac{33.5}{\delta[^\circ]}\right)\cdot\left(0.95\sin^2\frac{\delta}{2}+2.05\sin^4\frac{\delta}{2}\right)\right]+\frac{A_\delta}{\mathrm{Re}_\delta} \quad (11)$$

$$\mathrm{Re}_\delta = \frac{\rho b V_\delta}{\mu} \quad (12)$$

Coefficients $k_{\delta 1}$ and A_δ for sharp elbows depend on the angle of the turn. Empirical values are given for certain angles [10]. Using these values the appropriate interpolation was utilized in order to obtain $k_{\delta 1}$ and A_δ for the current geometries, as shown in Table 2. Given that the plenums have twice the height of the core flow channels entering or leaving, it is assumed that the volumetric flow of the fluid required to turn in this region is one half the total volumetric flow rate. As a result, the velocity of the fluid required to turn can be determined as:

$$V_\delta = \frac{\dot{V}/2}{NA_{ch}} \quad (13)$$

$$N = \text{number of channels} = \begin{cases} 5, \text{ heat sink A, B} \\ 4, \text{ heat sink C, D} \end{cases} \quad (14)$$

Table 1. CORRECTION FACTOR FOR THE ASYMMETRIC SUDDEN CHANGE OF FLOW AREA, k_1

expansion/contraction	heat sink	B/H	k_1
fitting–plenum	A	$\cong 3$	$\cong 0.9$
fitting–plenum	C,D	$\cong 2$	$\cong 0.95$
plenum to core channels	A,B,C,D	$= 2$	$\cong 0.95$

Table 2. COEFFICIENTS k_δ AND A_δ

$\delta[^\circ]$	$k_{\delta 1}$	A_δ
30	6	133
90	1.3	400
120	0.819	533

The loss coefficient through the Z bend, Δp_{Z-bend}, consists of two 90° bends, and is accordingly calculated as:

$$K_{Z-bend} = \frac{\Delta p_{Z-bend}}{\frac{1}{2}\rho V_Z^2} = 2 \cdot K_{\delta=90^\circ} \tag{15}$$

$$V_Z = V_{ch} = \frac{\dot{V}/N}{A_{ch}};\ \mathrm{Re}_{ch} = \frac{\rho b V_{ch}}{\mu} \tag{16}$$

The velocity through the Z bend (V_Z) and through the core channels (V_{ch}) are the same.

The pressure loss due to the fluid shear through a square channel of length L_{ch}, Δp_{ch}, in the core is determined using Muzychka's model [13] for the apparent Fanning friction factor (f_{app}) in Hydrodynamically Developing Flow (HDF) through the plain duct, of length L_{ch} and cross sectional area A_{ch}. The developing lengths for hydrodynamic and thermal boundary layers in straight ducts with constant cross-sectional area can be determined as [13]:

$$L_{hy} \approx 0.05 D_h \mathrm{Re}_{D_h};\ L_{th} \approx 0.05 D_h \mathrm{Re}_{D_h} \mathrm{Pr} \tag{17}$$

This criteria clearly shows that for the flow rates used in this research, both the hydrodynamic and thermal boundary layers remain in the developing region. It should be noted that in developing the formulations of friction factor Muzychka [13] used the square root of the cross sectional area as the characteristic length. In the case of the square cross section, this provides the same characteristic length, b, as one would obtain if the hydraulic diameter was used as the characteristic length.

The pressure drop model is based on the product of the apparent Fanning friction factor and the Reynolds number. This product in turn is determined using superposition of two asymptotic solutions for developing and fully developed flow as shown in Eq. (18). The actual weighting of these two solutions is self-determined based on the magnitude of the flow characteristics of the channel.

$$f_{app}\mathrm{Re}_{\sqrt{A}} = \left\{ \left(\frac{3.44}{\sqrt{z^+_{\sqrt{A}}}} \right)^2 + \left(f\mathrm{Re}_{\sqrt{A}} \right)^2 \right\}^{\frac{1}{2}} \tag{18}$$

$$f\mathrm{Re}_{\sqrt{A}} = \frac{12}{\sqrt{\varepsilon}(1+\varepsilon)\left[1 - \frac{192\varepsilon}{\pi^5}\tanh\left(\frac{\pi}{2\varepsilon}\right)\right]} \tag{19}$$

$$z^+_{\sqrt{A}} = \frac{z}{\sqrt{A}\mathrm{Re}_{\sqrt{A}}}, \text{nondimensional length} \tag{20}$$

$$z = L_{ch} = \begin{cases} 72\ mm \text{ for heat sinks A, B} \\ 57\ mm \text{ for heat sinks C, D} \end{cases} \tag{21}$$

$$\varepsilon = 1, \text{ aspect ratio of } A_{ch} \tag{22}$$

The connection between Fanning friction factor and pressure drop for plain duct flow is through the average shear stress:

$$f_{app} = \frac{\overline{\tau}_w}{\frac{1}{2}\rho V_{ch}^2};\ \Delta p_{ch} \cdot A_{ch} = \overline{\tau}_w \cdot A_{S-ch} \tag{23}$$

$$A_{S-ch} = L_{ch} \cdot 4 \cdot b \tag{24}$$

Therefore:

$$\Delta p_{ch} = \left(f_{app} \cdot \frac{1}{2}\rho V_{ch}^2 \right) \cdot \frac{A_{S-ch}}{A_{ch}} \tag{25}$$

Nondimensional Fanning friction - Reynolds Number Group of Heat Sinks Once the total pressure drop, Δp_{tot}, is determined by combining all the pressure drops in the flow path shown in Fig. 6, a dimensionless form of the overall Fanning friction factor can be obtained as follows:

$$f = \frac{\overline{\tau}_w}{\frac{1}{2}\rho \overline{V}_{ch}^2};\ \overline{\tau}_w \frac{A_{tot}}{N} = \Delta p_{tot} A_{ch} \tag{26}$$

A simple comparison of the various pressure drops in the flow path indicates that the majority of the flow resistance is in the core, with the predominant resistance being the resistance associated with the turning of the flow in Z-bends. As a result the overall Reynolds number will be based on the characteristic length of these channels, i.e.:

$$\mathrm{Re}_{\sqrt{A_{ch}}} = \mathrm{Re}_{ch} = \frac{\rho b V_{ch}}{\mu} \tag{27}$$

Comparison of Hydrodynamic Model with Data Predicted values of the hydrodynamic performance for four liquid cooled heat sinks: A, B,C and D are compared with the corresponding experimental values in Figs. 8 to 11 (the error bars show the maximum model - data discrepancy).

The pressure drop model reveals that the highest pressure loss occurs in the Z-bend (Δp_{Z-bend}), where the fluid flows from one plate of the heat sink to another, making two sharp 90° turns. This pressure loss comprises approximately $30\% - 40\%$ of the total loss, depending on the size of the heat sink.

The second largest local loss is due to the sudden expansion from the fitting into the inlet plenum, $\Delta p_{E-pl} \simeq 15 - 24\%$. The sudden contraction loss from the plenum to the fitting, Δp_{C-pl} ranges from $8 - 13\%$. The magnitude of these contraction/expansion losses is directly proportional to the size of the transition in the flow path.

Other significant flow losses can be attributed to turning in the entry and exit to and from the plenums, where $\Delta p_{\delta-turn}$ is of order 5% (or 10% overall for both entry and exit losses) and

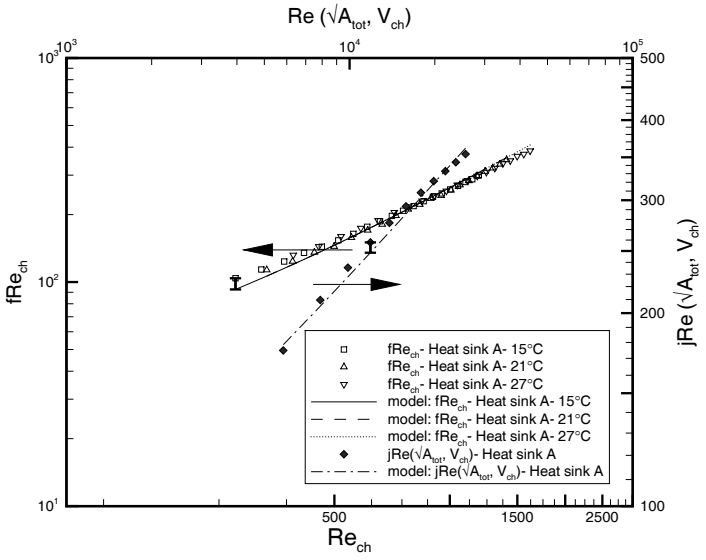

Figure 8. HEAT SINK A

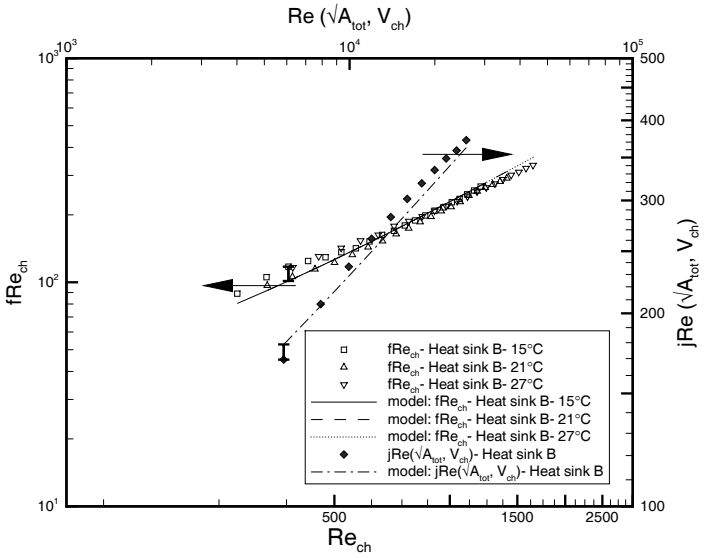

Figure 9. HEAT SINK B

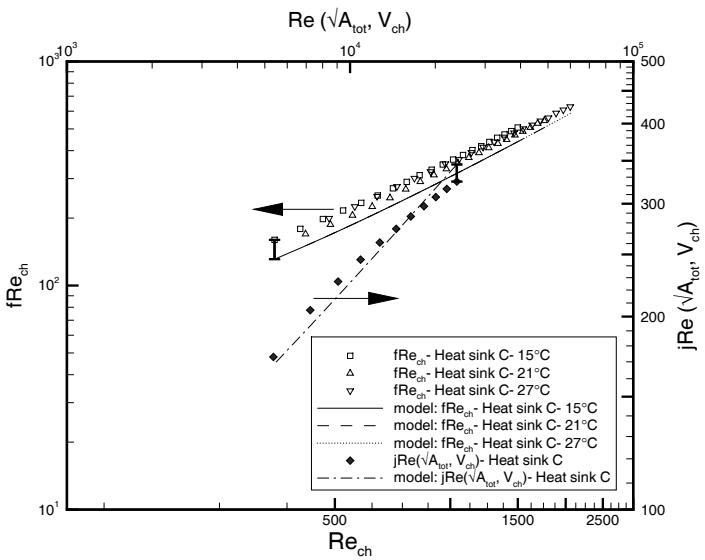

Figure 10. HEAT SINK C

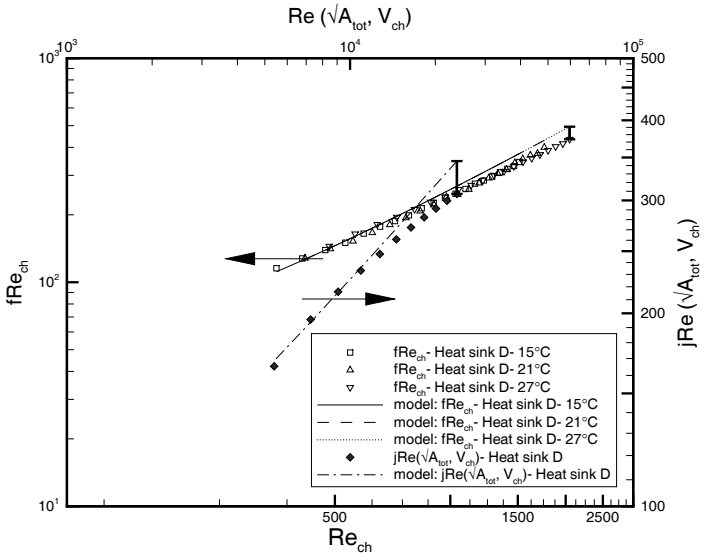

Figure 11. HEAT SINK D

contraction/expansion losses in the fitting, Δp_{C-fitt} and Δp_{E-fitt}, which contribute $5-8\%$ of the overall pressure drop.

Contraction and expansion losses from the plenum to the core, and vice versa, are almost negligible $(2-3\%)$. Channel friction loss contributes approximately $6-13\%$ to the total pressure drop, and since we have the case of hydrodynamically developing flow through the core channel of length L_{ch}, this loss is greater for the shorter channels in heat sinks C and D, compared to longer channels in heat sinks A and B.

Thermal Model

The thermal performance of the heat sinks is modeled based on a steady state analysis using a uniform wall temperature boundary condition. The overall convective heat transfer rate in the wetted interior of the heat sink can be predicted using the following:

$$
\begin{aligned}
Q_{tot} &= \rho \dot{V} C_p (T_{out} - T_{in}) \qquad (28)\\
Q_{tot} &= Q_{core} + 2Q_{plenum}\\
\overline{h}_{tot} A_{tot} \Delta T_{lm} &= \overline{h}_{ch} A_{core} \Delta T_{lm} + 2\overline{h}_{pl} A_{s-pl} \Delta T_{lm}\\
\overline{h}_{tot} A_{tot} &= \overline{h}_{ch} A_{core} + 2\overline{h}_{pl} A_{s-pl}
\end{aligned}
$$

$$\overline{h}_{tot} = \overline{h}_{ch}\frac{A_{core}}{A_{tot}} + \overline{h}_{pl}\frac{2A_{s-pl}}{A_{tot}}$$

where:

T_S = the UWT of wetted surface area of the heat sink
A_{tot} = total heat transfer surface area = $A_{core} + 2A_{s-pl}$
A_{core} = surface area of the core
A_{s-pl} = surface area of one plenum
$\overline{h}_{ch}$ = average heat transfer coefficient in core channels
$\overline{h}_{pl}$ = average heat transfer coefficient in plenums

The plenum surfaces, A_{s-pl}, are shown in the shaded regions in Fig. 12, while the remaining unshaded regions represent the core surface area, A_{core}. Heat transfer coefficients for the plenum and the core have been determined using the Nusselt number model for the Simultaneously Developing Flow (SDF) through plain ducts, developed by Muzychka [14]. The plenums are approximated as straight rectangular ducts with dimensions $W_{plenum} \times H_{plenum} \times L_{plenum}$. Despite this approximation the actual surface area of the plenum is preserved and can be calculated as:

$$A_{s-pl} = 2 \cdot (W_{plenum} + H_{plenum}) \cdot L_{plenum} \tag{29}$$

Because of the repeated overlapping flow channels in the core a fundamental unit cell was identified as shown in Fig. 13. The basic feature of this unit cell is a flow channel of cross sectional area, A_{ch}, and flow length, l_{ch}. While there are minor differences in the flow length throughout the core, a single averaged value was obtained to represent the length of the short channel in the core.

The heat transfer model for forced convection in the combined entry region of plain ducts, developed by Muzychka [14] is:

$$Nu_{\sqrt{A}}(z^*) = \left[\left(\left\{ C_1 C_2 \left(\frac{f\mathrm{Re}_{\sqrt{A}}}{z^*_{\sqrt{A}}} \right)^{1/3} \right\}^5 + \left\{ C_3 \left(\frac{f\mathrm{Re}_{\sqrt{A}}}{8\sqrt{\pi}\varepsilon^{\gamma}} \right) \right\}^5 \right)^{m/5} + \left(\frac{C_4 f(\mathrm{Pr})}{\sqrt{z^*_{\sqrt{A}}}} \right)^m \right]^{1/m} \tag{30}$$

where, for isothermal walls (UWT) the constants are:

$$C_1 = \frac{3}{2}; C_2 = 0.409; C_3 = 3.24; C_4 = 2 \tag{31}$$
$f\mathrm{Re}_{\sqrt{A}}$, see Eq. (19)

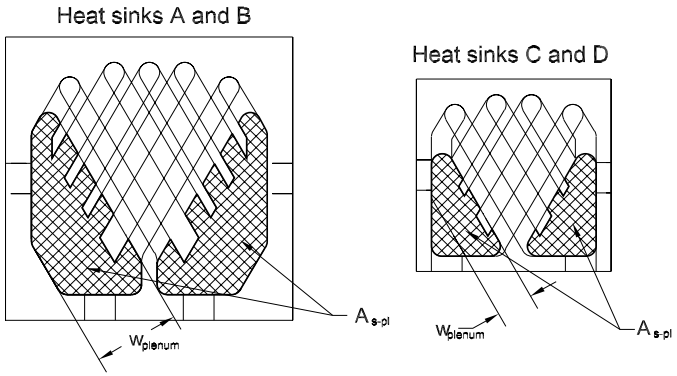

Figure 12. SURFACE AREAS OF HEAT SINKS' PLENUMS (SHADED AREA)

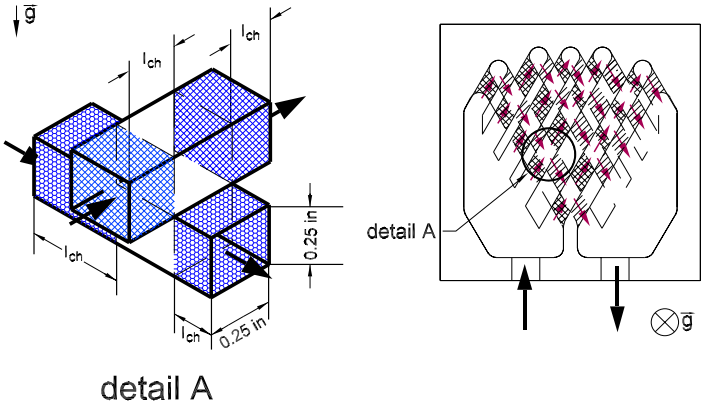

Figure 13. THE SHORT CHANNEL, l_{ch}, IN THE CORE

$$f(\mathrm{Pr}) = \frac{0.564}{\left[1 + (1.664\,\mathrm{Pr}^{1/6})^{9/2}\right]^{2/9}} \tag{32}$$

$$m = 2.27 + 1.65 \cdot \mathrm{Pr}^{1/3}, \text{ for } 0.1 < \mathrm{Pr} < 1000 \tag{33}$$

$$z^* = \frac{z}{\sqrt{A}\mathrm{Re}_{\sqrt{A}}\mathrm{Pr}}, \text{ nondimensional length} \tag{34}$$

$$z = \begin{cases} L_{plenum}, & \text{plenum channel length} \\ l_{ch}, & \text{core channel length} \end{cases} \tag{35}$$

The model presented in Eq. (30) was assembled by combining limiting solutions for three distinct regions, namely i) fully developed hydrodynamic flow, ii) developing thermal flow and iii) simultaneously developing thermal and hydrodynamic flow.

The velocity in the plenum is defined as:

$$V_{pl} = \frac{\dot{V}}{A_{c-pl}} = \frac{\dot{V}}{W_{plenum} \cdot H_{plenum}} \tag{36}$$

The velocity through the short channels in the core, assuming uniform distribution and no mixing of flows between the two plates, is equal to the channel velocity, V_{ch}, in hydrodynamic model, Eq.(16).

The corresponding heat transfer coefficients for the plenum and the core can be determined as:

$$h_{plenum} = \frac{Nu_{\sqrt{A_{c-pl}}} k_f}{\sqrt{A_{c-pl}}} \tag{37}$$

$$h_{ch} = \frac{Nu_{\sqrt{A_{ch}}} k_f}{\sqrt{A_{ch}}} \tag{38}$$

Back to Eq. (28), the total heat transfer coefficient, h_{tot} can be determined. The geometrical parameters are given in Table 3.

Table 3. GEOMETRICAL PARAMETERS

	heat sink	
	A,B	C,D
$A_{tot}[mm^2]$	17,806.3	9,685.5
$A_{s-pl}[mm^2]$	3,769.7	1,659.8
$W_{plenum}[mm]$	26.6	12
$l_{ch}[mm]$	5.8	5.9

Nondimensional Colburn j Factor – Reynolds Number Group of Heat Sinks Heat transfer performance can be presented in terms of the Colburn j factor (Shah and London, [15]), given as:

$$j = \frac{\overline{Nu}}{\mathrm{Re}\,\mathrm{Pr}^{1/3}} \tag{39}$$

or more conventionally as

$$j\mathrm{Re} = \frac{\overline{Nu}}{\mathrm{Pr}^{1/3}} \tag{40}$$

For complex geometries such as those studied in this work, a single characteristic length may be difficult to identify. Yovanovich [16] has shown that the square root of the wetted surface area provides as effective characteristic length in most instances.

$$\overline{Nu}_{tot} = \frac{\overline{h}_{tot}\sqrt{A_{tot}}}{k_f} \tag{41}$$

The Colburn j factor Reynolds group is plotted against corresponding Reynolds number, which is defined as:

$$\mathrm{Re}_{\sqrt{A_{tot}}} = \frac{\rho\sqrt{A_{tot}}V_{ch}}{\mu} \tag{42}$$

with the velocity through the channels of the core (V_{ch}) as the characteristic velocity for the heat sink.

Comparison of Thermal Model with Data Figures 8 to 11 show the comparison of experimental data and the thermal model (the error bars show the maximum model–data discrepancy). The largest discrepancy between the model and the data occurs with heat sink D, where the RMS (root mean square) of relative percentage differences is 6.54%. At higher Reynolds numbers the trend of the data points substantially diverges from the straight line of the model, especially in case of smaller size heat sinks (C, D). It seems that with a significant increase of Reynolds number the thermal performance of the heat sinks would reach an asymptotic limit, which would occur faster in smaller heat sinks (C, D) since their curvature is pronounced than in heat sinks A and B.

According to the model prediction, $81-83\%$ of heat transfer to the coolant occurs in the core, while the inlet and outlet plenums are responsible for 8.5–9.5% of total heat transfer each. The heat transfer coefficient in the core's short channels (h_{ch}) is 2.3 to 3.7 times greater than the heat transfer coefficient in the plenum (h_{plenum}).

Most of the heat energy is transferred in the corrugated section of calistor, the core. It is recommended to decrease the participation of plenum surface area (A_{s-pl}) in total wetted surface area (A_{tot}) which would enhance the overall thermal performance of calistor.

SUMMARY

An experimental and analytical study of four liquid cooled heat sinks is presented. The thermal and hydrodynamic performances were considered separately and the results are summarized below. The agreement between the data and the models is within 15% RMS. The experimental tests have been conducted using 50/50 Water/Ethylene-glycol mixture, and flow rate range between 2.5 and 0.5 gpm. The hydraulic resistance network approach has been demonstrated as an effective means of determining the pressure losses within the flow path of the heat sink. The thermal model used a general heat energy balance for the heat sink, while applying a geometrical simplification on the elements of its geometry, observing them as the plain duct flows.

The analysis suggests that it would be beneficial for overall hydrodynamic and thermal performance if the flow velocity in the core channels was lower, reducing the pressure drop, and the length l_{ch} shorter, enhancing heat transfer coefficient in the core. For example, the modified – smaller – rib width, assuming the same A_{ch}, would provide more channels in the core with lower velocities and larger heat transfer area and shorter lengths (l_{ch}).

ACKNOWLEDGMENT

The support of Ferraz Shawmut Inc., who provided engineering guidance, numerous heat sink samples for the experimental test program, as well as financial support of the research study, is gratefully acknowledged. The authors would also like to thank Materials and Manufacturing Ontario (MMO) for their continued financial support of this research.

REFERENCES

[1] Baumann, H., Heinemeyer, P., Staiger, W., Topfer, M., Unger, K., and Muller, D., "Optimized Cooling Systems for High-Power Semiconductor Devices," *IEEE Transactions on Industrial Electronics,* Vol. 48, No. 2, pp. 298 - 306, 2001

[2] Agonafer, D., Han, Z.-X. and Schmidt, R., "Numerical Prediction of the Thermal Resistance of Cold Plate," *Intersociety Electronic Packaging Technical/Business Conference and Exhibition,* July 8 - 13, Kauai, HI, *Advances in Electronic Packaging,* Vol. 2, pp. 983 - 987, 2001.

[3] Stasiek, J., Collins, M.W., Ciofalo, M. and Chew, P.E., "Investigation of flow and heat transfer in corrugated passages-Experimental results, " *International Journal of Heat and Mass Transfer,* Vol. 39, No. 1, pp. 149 - 164, 1996.

[4] Ciofalo, M.,Stasiek, J. and Collins, M.W., "Investigation of flow and heat transfer in corrugated passages-Numerical simulations," *International Journal of Heat and Mass Transfer,* Vol. 39, No. 1, pp. 165 - 192, 1996.

[5] Focke, W.W., Zachariades, J. and Olivier, I., "The effect of the corrugation inclination angle on the thermohydraulic performance of plate heat exchangers, " *International Journal of Heat and Mass Transfer,* Vol. 28, No. 8, pp. 1469 - 1479, 1985.

[6] Okada, K., Ono, M., Tomimura, T., Okuma, T., Konno, H. and Ohtani, S., "Design and Heat Transfer Characteristics of New Plate Heat Exchanger," *Heat Transfer-Japanese Research,* Vol. 1, No. 1, pp. 90 - 95, 1972.

[7] Blomerius, H.,Hosken, C. and Mitra, N.K., "Numerical Investigation of Flow Field and Heat Transfer in Cross-Corrugated Ducts," *Transactions of the ASME: Journal of Heat Transfer,* Vol. 121, pp. 314 - 321, 1999.

[8] Rosenblad, G. and Kullendorf, A., "Estimating Heat Transfer Rates from Mass Transfer Studies on Plate Heat Exchanger Surfaces," *Warme und Stoffubertragung,* Vol. 8, pp. 187 - 191, 1975.

[9] Croce,G. and D'Agaro, P., "Numerical analysis of forced convection in plate and frame heat exchangers," *International Journal of Numerical Methods for Heat and Fluid Flow,* Vol. 12, No. 6, pp. 756 - 771, 2002.

[10] Idelchik, I.E., *Handbook of Hydraulic Resistance,* CRC Press, FL, 1990.

[11] Blevins, R.D., *Applied Fluid Dynamics Handbook,* Van Nostrand Reinhold Company Inc., New York, 1984.

[12] White, F.M., *Fluid Mechanics,* McGraw-Hill,Inc., New York, 1994.

[13] Muzychka, Y.S., "Analytical and Experimental Study of Fluid Friction and Heat Transfer in Low Reynolds Number Flow Heat Exchangers," Ph.D. Thesis, Department of Mechanical Engineering, University of Waterloo, Waterloo, Ontario, Canada, 1999.

[14] Muzychka, Y.S. and Yovanovich, M.M., "Laminar Forced Convection Heat Transfer in the Combined Entry Region of Non-Circular Ducts," *Journal of Heat Transfer,* Vol. 126, 2004.

[15] Shah, R.K. and London, A.L., *Laminar Flow Forced Convection in Ducts,* Academic Press, New York, 1978.

[16] Yovanovich, M.M., "New Nusselt and Sherwood Numbers for Arbitrary Isopotential Geometries at Near Zero Peclet and Rayleigh Numbers," *AIAA 22nd Thermophysics Conference,* Honolulu, HI, June 8 - 10, 1987.